Journal of Materials Chemistry A

ROYAL SOCIETY OF CHEMISTRY

REVIEW

View Article Online
View Journal | View Issue

Cite this: J. Mater. Chem. A, 2025, 13, 30755

Reasonable active site design for promoting water dissociation and carbon monoxide activation in a low-temperature water-gas shift reaction

Shikun Wang,[ab] Shuangde Li,*[ab] Linfeng Nie[a] and Yunfa Chen *[ab]

To solve the energy crisis, the water–gas shift reaction (WGSR) has been systematically studied for the effective production of pure hydrogen and removal of hazardous carbon monoxide. In typical industrial applications, the WGSR commonly consists of two individual processes: a high-temperature shift reaction (320–450 °C) for a high reaction rate and a low-temperature shift reaction (150–300 °C) for high conversion due to their intrinsic thermodynamic and kinetic properties. Owing to the complexity of a traditional catalytic system, researchers have made great efforts to seek low-temperature (<300 °C) reaction catalysts with better performance and energy efficiency. Recent advancements have mainly focused on the correlation of the catalyst components and reactivities for low-temperature WGSR. In contrast, this work considers different catalyst design ideas for enhancing the low-temperature WGSR performance based on the combination of two half-reactions, namely, water dissociation and carbon monoxide activation, which occur on different active sites. Therefore, only an intentional design of the active sites for the two half-reactions can constitute an efficient catalyst. This review aims to summarize the advances made in the recent decade and provides some direction toward possible active site designs for future investigation.

Received 12th March 2025
Accepted 29th July 2025

DOI: 10.1039/d5ta02030a

rsc.li/materials-a

1 Introduction

Hydrogen (H_2) is widely recognized as a potential clean energy carrier that may help reduce greenhouse gas emissions. A number of hydrogen production processes have been developed and studied by scientists. Among them, the water–gas shift reaction (WGSR) is considered an efficient way to produce and purify H_2.1 It has been applied to many industrial processes, such as natural gas reforming, ammonia synthesis[2] and fuel cell applications.[3,4]

The history of the WGSR can be traced back to the 1780s, and its reaction is depicted in the following equation: $CO + H_2O \leftrightarrow CO_2 + H_2$ ($\Delta H_r^{\theta} = -41.1$ kJ mol^{-1}). As an exothermic reaction, it is thermodynamically suitable at low temperatures with strict kinetic limits. Therefore, the conventional WGSR system contains two adiabatic stages: a high-temperature stage with an Fe–Cr catalyst for a high reaction rate and a low-temperature stage with a Cu–Zn–Al catalyst (<300 °C) for the forward conversion.[5,6] The reaction was not applied until 1888 when Mond utilized it for hydrogen production for fuel cell application. In 1914, Bosch and Wild applied the reaction in the industrial production of hydrogen.[7] Because of the toxicity of Cr and the high energy consumption, scientists struggled to optimize the performance of Fe-based catalysts by introducing different kinds of adjuvants until the 1980s.[8] However, the complexity and energy consumption of the system still motivated scientists to develop new catalytic systems.

Encouraged by the proposal of an associative mechanism and redox mechanism in 1920 and 1940,[1] scientists realized that the reaction is mainly induced by the interfacial sites between loaded metals and the supports on heterogeneous catalysts.[9] Increasing kinds of metal oxides have been revealed to have decent water dissociation performance and mild reaction conditions, such as Al_2O_3,[10,11] $CuFe_2O_4$,12 ZrO_2,13 and $CeZrO_4$.14 Also, the catalytic performance can be assisted by additives such as ZnO,[15] Nb_2O_5,16 which adjust the physical properties and electronic structure of the catalysts. Besides metal oxides, some advanced functional materials were noted by researchers for their exclusive properties. For example, noble metal-based catalysts with α-MoC as a carrier were investigated in the last few years for their excellent water dissociation activity.[17]

With the development of catalyst design strategies,[18] noble metal-based catalysts have attracted much attention in this field.[19,20] With their moderate adsorption capacity for CO, metals like Au, Pt, Ru, Pd, and Ag are frequently selected as active components for WGSR.[21,22] Furthermore, in 2011, Zhang *et al.* firstly realized a single atom catalyst (SAC) that consisted

[a]State Key Laboratory of Mesoscience and Engineering, Institute of Process Engineering, Chinese Academy of Sciences, Beijing 100190, People's Republic of China. E-mail: sdli@ipe.ac.cn; chenyf@ipe.ac.cn

[b]University of Chinese Academy of Sciences, No. 19A Yuquan Road, Beijing 100049, People's Republic of China

of single Pt atoms uniformly dispersed on a FeO_x support.[23] With their decent catalytic activity and new reaction mechanisms, SACs were further explored for better synthesis methods and catalytic properties, and regarded as promising catalysts for WGSR.[24] However, in some occasions, the nanoparticles showed significant catalytic activity, whereas the single atoms acted as spectators.[25] Thus, it is necessary to differentiate the function of nanoparticles and single atoms in different catalyst systems for CO activation.

Up to now, most WGSR reviews have mainly focused on the correlation between different catalyst structures and performances, like noble metal catalysts, transitional metal-based composites and others. For example, Zhou *et al.* discussed different sorts of supported metal nanoparticle catalysts for WGSR,[1] and Chen *et al.* provided a detailed summary of noble metal-based single-atom catalysts for WGSR.[21] Pal *et al.* provided a systematic review for transitional metal-based catalysts,[26] and Lee *et al.* focused on the impacts of reaction conditions and catalysts on WGSR involving different feed gases.[27] Some other reviews with their perspectives and proposed catalyst and active site design approaches have been summarized in Table 1. These reviews demonstrated the comprehensive understanding of different catalytic systems, and summarized the promising catalysts in terms of material composition. However, to our best knowledge, few reviews provided a discussion based on an understanding of designing the active site. This motivated us to summarize the first-class catalyst designs, and attempt to find some possible correlation between the active site structure and promising catalytic performance. More importantly, based on the proposal of surface catalytic theory[28] and the specificity of the WGSR, this review considers it as a combination of two principal half-reactions: water dissociation and CO activation. This review also emphasizes that most of the excellent catalyst design strategies focus on at least one of the half-reactions, whose importance was hardly acknowledged in previous reviews, as shown in the last row of Table 1. Additionally, with the knowledge that the deactivation of catalysts is still an inevitable phenomenon under actual situations, some active site design strategies were directed toward inhibiting deactivation, which is worth discussing with their specific examples in this review.

2 Mechanisms

Studies on the mechanism of WGSR have been conducted for a few decades because it is complex and still remains controversial. The most recognized mechanisms can be roughly divided into two categories, mainly involving different routes of water dissociation and carbon monoxide activation: redox mechanism and associative mechanism.

The redox mechanism was first proposed by Temkin in 1949.[29] The shift reaction goes through a redox cycle, as shown in the schematic in Fig. 1a and eqn (1)–(5), where * represents the active site. More specifically, H_2O will be directly adsorbed and activated on the active sites to be thoroughly dissociated into H_2 and O* (light blue balls: H atoms; dark blue balls: O atoms; dashed circle: oxygen vacancy; grey rectangle: support) and consume much energy. Simultaneously, CO will be activated and react with the lattice oxygen to generate CO_2, leaving an oxygen vacancy which will be supplied by the O* from H_2O (black balls: C atoms; light yellow balls: low valence state noble metals; dark yellow balls: high valence state noble metals; yellow ellipse: noble metal sites). The reduction process is entirely independent from CO oxidation, and needs enough activation energy to be thoroughly dissociated. Therefore, this mechanism is more favored by the high-temperature shift reaction and active sites with better reduction capacity.

$$H_2O + * \rightarrow H_2O^* \rightarrow H^* + {}^*OH \rightarrow 2H^* + O^* \quad (1)$$

$$O^* + O_V \rightarrow O_L \quad (2)$$

$$2H^* \rightarrow H_2 \quad (3)$$

$$CO + * \rightarrow CO^* \quad (4)$$

$$CO^* + O_L \rightarrow CO_2 + O_V \quad (5)$$

With the research trend for the lower reaction temperature, the associative mechanism based on the Langmuir–Hinshelwood model has gradually attracted much attention. As shown in the schematic in Fig. 1b, different from the redox mechanism, the water dissociation will only be partially dissociated into H* and *OH. The *OH will further react with CO* to generate important free radical intermediates, such as carboxyl (*COOH) and formyl (HCOO*). Thus, the reduction and oxidation processes are not independent, but associative. The intermediates will decompose into CO_2 and an extra H*, which can combine with the former H* to produce H_2. This mechanism described by eqn (6)–(9) revealed that the *OH could directly react with activated CO and form important intermediates, which could be further reformed into CO_2 and H_2, rather than undergo indispensable exhaustive dissociation into O* and H* with higher activation energy, resulting in a lower reaction temperature.

$$H_2O + * \rightarrow H_2O^* \rightarrow H^* + {}^*OH \quad (6)$$

$$CO + * \rightarrow CO^* \quad (7)$$

$$CO^* + {}^*OH \rightarrow {}^*COOH \rightarrow CO_2 + H^* \text{ (carboxyl-intermediate pathway)} \quad (8.1)$$

$$CO^* + {}^*OH \rightarrow HCOO^* \rightarrow CO_2 + H^* \text{ (formyl-intermediate pathway)} \quad (8.2)$$

$$2H^* \rightarrow H_2 \quad (9)$$

Both mechanisms above could be plausible under different conditions with different rate-determining steps (RDS). For example, WGSR on classic high-temperature catalysts like the Fe_3O_4 composite tends to follow the redox mechanism. Huang *et al.* conducted a detailed density functional theory calculation using the Fe_3O_4 (111) surface with the $Fe_{oct2\text{-}tet1}$ terminal, and proved that the redox mechanism was the primary reaction route with the RDS of CO_2 desorption because of the

Table 1 Summary of the review perspectives and proposed catalyst and active site design approaches of some published reviews and this work

Title	Published year	Review perspective	Proposed catalyst and active site design approach	Ref.
For more and purer hydrogen-the progress and challenges in water gas shift reaction	2023	Catalyst type and catalyst structure	Low and high temperature shift reaction catalysts Sulfur-tolerant and wide temperature shift reaction catalysts Nano catalysts and single-atom catalysts design Surface structure design	1
The water gas shift reaction: catalysts and reaction mechanism	2021	Catalyst component	Fe-based catalysts Cu-based catalysts Ni-based catalysts Co/Mo-based catalysts Noble metal-based catalysts	8
Noble metal-based single-atom catalysts for the water-gas shift reaction	2021	Catalyst component and active species (noble metal-based catalysts)	Single-atom catalysts with reducible oxide, irreducible oxide, carbides and nitride supports Active metal species (positive state and metallic state)	21
Platinum-based catalysts in the water gas shift reaction: recent advances	2020	Catalyst component and mechanism study (platinum-based catalysts)	The influence of supports The influence of the loading method and loading amount The influence of the promoter addition Kinetic and mechanism study of Pt-based catalysts	22
The review of Cr-free Fe-based catalysts for high-temperature water-gas shift reactions	2013	Catalyst component (Fe–Cr-based catalysts)	Iron oxide-chromium oxide catalysts Chromium-free catalysts	7
Water gas shift catalysis	2009	Catalyst component	Iron oxide-chromium oxide and chromium free catalysts for the high-temperature shift reaction Cu–Zn–Al and promoted Cu catalysts for low-temperature shift reaction Sulfur-tolerant catalysts Noble-metal-based catalysts Monolith-coated catalysts for fuel cell	
The water–gas shift reaction	2006	Catalyst component and kinetic study	Iron-based shift catalysts Copper-based shift catalysts Cobalt molybdenum-based shift catalysts	6
Reasonable active site design for promoting water dissociation and carbon monoxide activation in a low temperature water-gas shift reaction	—	Mechanism summary and active-site-design strategy for the two half-reactions of WGSR	Mechanism study of WGSR Active site design strategies for H_2O dissociation Active site design strategies for CO activation	This work

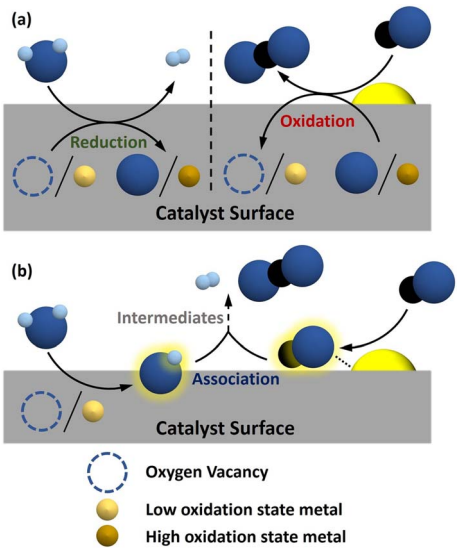

Fig. 1 (a) Process schematic of the redox mechanism. (b) Process schematic of the associative mechanism.

distinguishing water adsorption ability of the Fe_{oct2} sites.[30] Nevertheless, noble metal catalysts with abundant well-designed interfacial active sites allowed for the easy combination of CO* and *OH, leading to the associative mechanism. Vecchietti *et al.* studied the Pt/CeO_2 catalyst *via* diffuse reflectance infrared Fourier transform spectroscopy (DRIFTS). Their results demonstrated the existence of HCOO* and COO* species, which are typical intermediates of the associative mechanism. They also mentioned that in contrast to the previous research, the activation of water molecules in the WGSR mechanism is not the RDS in this system.[31] These previous works emphasized the complexity of the reaction mechanisms with various catalytic systems, suggesting that the reasonable design of the interfacial site that initiates the associative mechanism might be a common solution for the first-class catalysts. Considering that the water dissociation and CO activation are both inevitable for WGSR, these two vital processes could be thinking pivots for future design strategies of the active site, which will be further discussed in the following section of the review.

3 Active site design

3.1 Water dissociation

Water dissociation is a key process of H_2 production and active intermediate generation in WGSR. Metal oxides have been widely studied in laboratories and industrial processes for water dissociation. As a kind of common defect site on the surface of oxide catalysts, oxygen vacancies are regarded as the reaction sites, and it has been extensively investigated because of its high activity and stability.[32] Mostly, the activity of oxygen vacancies can be influenced by two factors: concentration and species. Some metal sites can perform water dissociation by intentional catalyst design. Therefore, it is worthwhile to summarize the design ideas for active sites, which is shown in Fig. 2.

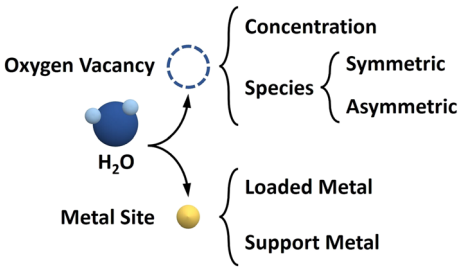

Fig. 2 Summary of the active site design for H_2O dissociation.

3.1.1 Oxygen vacancy

3.1.1.1 Concentration of the oxygen vacancy. For reducible metal oxide supports, such as CuO,[33] Fe_2O_3,[34] TiO_2,[35] CeO_2 (ref. 36) and others, the concentration of the oxygen vacancy can be easily controlled by synthesis and pretreatment methods, such as element doping. Jeong *et al.* prepared a series of $Cu–CeO_2–ZrO_2$ materials with different Ce/Zr ratios. They found that by shrinking the lattice, $Cu–Ce_{0.8}Zr_{0.2}O_2$ contained a larger amount of oxygen vacancies and exhibited very stable WGSR activity at about 300 °C, which is correlated with the enhancement of the oxygen mobility. This work also mentioned that compared with the tetragonal phase of $Cu–Ce_{0.8}Zr_{0.2}O_2$, the cubic phase shows higher WGSR activity because it helps to achieve a higher concentration of oxygen vacancy.[14] Homogeneously, the design of La-doped CeO_2 (ref. 37 and 38) and Ga-doped Pt/CeO_2 (ref. 31) achieved a high concentration of oxygen vacancies, thereby promoting the catalytic activity for WGSR. Therefore, element doping is regarded as a valid performance-promoting pathway.[39] Similarly, the synthesis condition of the catalysts can change the O_V concentration, which will be further discussed.

In summary, there are direct evidences showing that materials with more oxygen vacancies tend to be more active in the water dissociation process. This is because oxygen vacancies serve as the main active site of water dissociation and can stabilize the *OH, which enhance the WGSR activity.

3.1.1.2 Species of oxygen vacancy. Apart from gaining a higher concentration of oxygen vacancies, recent advanced works mainly focus on the species of oxygen vacancy. Zhou *et al.* successfully formed an asymmetric environment of oxygen vacancies by element doping.[32] For example, the group doped Bi in CeO_2 and modified the surrounding of the oxygen vacancy by forming a distorted tetrahedral geometry of $Bi–O_v–Ce_3$. In comparison with traditional symmetric clusters like $Ce_2–O_v–Ce_2$, the asymmetric oxygen vacancy facilitates both the adsorption and desorption processes (Fig. 3a).[40] It is predictable that such asymmetric oxygen vacancy can be applied to some structure-sensitive reactions like the activation of H_2O in WGSR.

Researchers obtained a Zn–Ti mixed oxide support from a Zn–Ti layered double hydroxide precursor. Because of the strong metal-support interaction, after loading Au nanoparticles, the electrons will transfer from the TiO_{2-x} overlayer to Au atoms to form the asymmetric oxygen vacancy site $Au^{\delta-}–O_v–Ti^{3+}$, as shown in Fig. 3b. An in-depth analysis of the X-ray

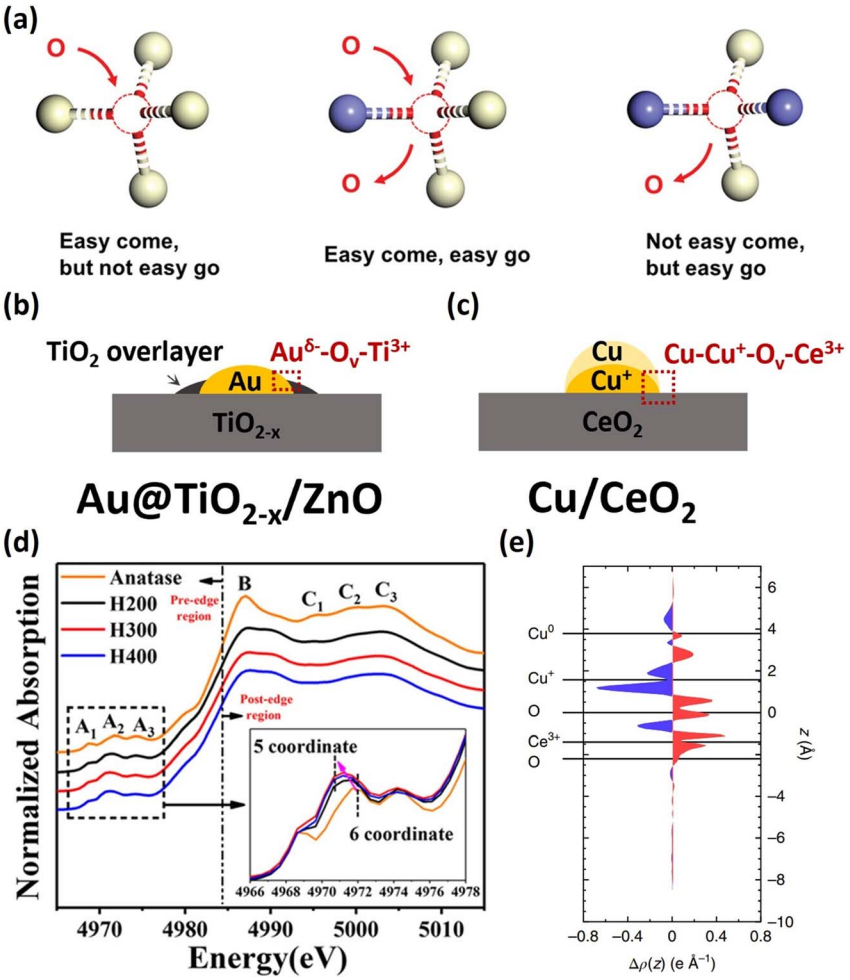

Fig. 3 (a) Schematic of the relationship between the microstructure of the oxygen vacancy and its redox property. (b) Diagram of the active site structure on Au@TiO_{2-x}/ZnO. (c) Diagram of the active site structure on Cu/CeO_2. (d) Normalized XANES spectra of Au@TiO_{2-x}/ZnO with different synthesizing conditions, providing direct evidence for the existence of an asymmetric oxygen vacancy site ($Au^{\delta-}$–O_v–Ti^{3+}). (e) Plane-integrated bonding charge $\Delta\rho(z)$ as a function of position across the Cu–Ce interface. Red and blue areas represent charge accumulation and depletion, respectively. (d) Copyright © 2019, American Chemical Society. (e) Copyright 2019, The Author(s), under exclusive license to Springer Nature Limited.

absorption near edge structure (XANES) results shown in Fig. 3d also provided convincing evidence of the asymmetric oxygen vacancies. During the WGSR, both $Au^{\delta-}$ and O_v species of the site directly participate in the H_2O dissociation process. Moreover, characterization results showed that the active oxygen vacancy also accelerated the CO chemisorption and H_2O dissociation.[41] The group also reported a TiO_{2-x}-modified Ni catalyst with tunable Ni–TiO_{2-x} interaction, and the reaction process over $Ni^{\delta-}$–O_v–Ti^{3+} site was discussed. By the *in situ* time-resolved DRIFTS results, a new redox mechanism was revealed, which can be illustrated by two main steps: (1) the cleavage of the O–H bond in the H_2O molecule at the asymmetric oxygen vacancy site to generate H_2 and transform $Ni^{\delta-}$–O_v–Ti^{3+} into $Ni^{\delta+}$–O–Ti^{4+}; (2) the reaction between CO and $Ni^{\delta+}$–O–Ti^{4+} to form CO_2 and $Ni^{\delta-}$–O_v–Ti^{3+}. These works focus on the establishment of an asymmetric active oxygen vacancy, and provide a new possible solution for the construction of high-efficiency heterogeneous catalytic systems.[42,43] Many other works have successfully synthesized composites with asymmetric oxygen vacancies, which also exhibited LT-WGSR performance.[44]

Additionally, based on the design of the asymmetric oxygen vacancy, Chen *et al.* synthesized a bilayer Cu covered on CeO_2 (structure illustrated in Fig. 3c). The bottom layer of Cu can donate an electron to Ce^{4+} and coordinate with an O_v to form a Cu^+–O_v–Ce^{3+} site, and the top layer of Cu can bond with the underlying Cu^+ to modify the site to Cu^0–Cu^+–O_v–Ce^{3+}. Such interfacial active sites can optimize the plane-integrated bonding charge shown in Fig. 3e around the Cu^+ and O_v sites, thereby enhancing the CO adsorption and H_2O dissociation capacity.[45]

Although the oxygen vacancy concentration is an important factor for the catalytic performance, its optimization is capped by the stability requirement of catalysts. Designing better oxygen vacancy species like the asymmetric oxygen vacancy is more crucial for achieving a more efficient catalytic system, and can fundamentally reveal the H_2O dissociation mechanism.

3.1.2 Metal site. Except for oxygen vacancies, metal sites can also serve as the core sites for water dissociation. For traditional metal oxide catalysts, the loaded metal can be the water adsorption sites, and the dissociation capacity can be enhanced by the establishment of interfaces between loaded metals and supports. Lucas *et al.* designed a Ni/Al_2O_3 composite and closely tracked the oxygenate species (O* and *OH) from the water dissociation process at interface sites in contrast to the bare Ni surface. They found that the surface species are only available at the interfacial sites. The results demonstrated that the combination of a metal and support can be properly adjusted to obtain better water dissociation activity, and the WGSR is a typical interface–sensitive reaction.[11]

Many studies center on MoC for the production of high-purity H_2 have been carried out and achieved intriguing advances.[46,47] Other oxides, like SiO_2 or TiO_2, cannot dissociate H_2O or can easily dissociate H_2O into H^+ and OH^-, respectively. Mass spectral results have shown that after being adsorbed on α-MoC, H_2O can be instantly dissociated into H* and *OH at almost room temperature, which are both important intermediates for WGSR.[48] Researchers composed a review to summarize the efforts they made on the development of M/MoC. The review mentioned that the exceptional catalytic performance of MoC originated from the incorporation of carbon atoms at the interstitial sites, which endows MoC with higher density of states near the Fermi level and proper electronic interaction between carbon atoms and metals. Such electronic interaction can optimize the adsorption energy of H_2O to a moderate level, where the H_2O molecule can be solidly adsorbed on the surface and simultaneously dissociated by the energy released from adsorption.[49] Furthermore, Zhang *et al.* designed Pt_1–Pt_n/α-MoC (morphology and structure shown in Fig. 4a) based on Pt_1/α-MoC with promising activity but disappointing stability, and obtained better CO conversion than the Cu–Zn–Al model catalyst and other MoC-based catalysts given in Fig. 4b. The extra Pt clusters can change the interfacial structure by covering the redundant exposed surfaces of Pt_1/α-MoC to prevent the oxidation of α-MoC by the excess *OH, because the *OH is far from the interface of Pt and α-MoC cannot react with the activated CO. Furthermore, transient kinetic analysis (TKA) of Pt_1–Pt_n/α-MoC revealed that except for H_2O dissociation, CO can also be dissociated at low temperature to generate an extra carbon atom, which can then react with activated H_2O to produce an additional 35% of H_2 in the total H_2 production yield. The reaction routes are summarized in Fig. 4c. Using the isotope labelling method, this work found some different

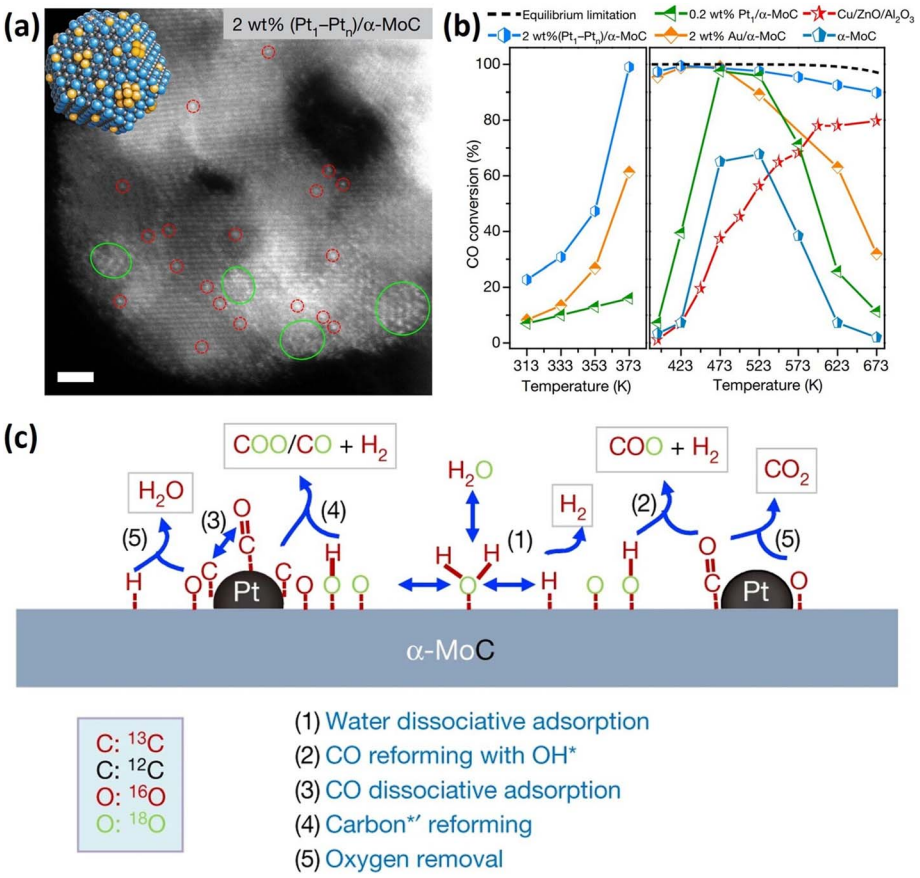

Fig. 4 (a) TEM image and a diagram of the distribution of Pt single atoms and clusters on (Pt_1–Pt_n)α-MoC. (b) CO conversion over different catalysts at various temperatures. (c) Schematic of the reaction routes for the WGS reaction over Pt/α-MoC: (1) water dissociation; (2) the conventional WGS reaction routes (redox or associative intermediate mechanism); and (3)–(5) the unconventional WGS reaction routes. The asterisk represents the active site. Copyright 2021, The Author(s), under exclusive license to Springer Nature Limited.

reaction routes based on the dissociation of CO. This meant that the combination of a noble metal and α-MoC can not only make full use of the water dissociation capacity of MoC, but also enhance the CO activation process, resulting in a greater active oxygen species supplement from CO dissociation.[50] The exceptional performance of α-MoC-based catalysts provides a possibility for future research to investigate the electronic structure optimization of metal sites to improve their intrinsic H_2O dissociation ability, but there might be still many challenges to improving the current performance of the α-MoC-based catalysts.

MoC has been proved as an outstanding H_2O dissociation material. Other carbides like TiC[51,52] and Co_2C[53] are also under investigation. Additionally, metal–organic frameworks (MOFs) have been predicted as promising supports with a controllable porous structure and changeable open metal sites (OMSs).[54] However, there have been limited MOFs applied in LT-WGSR because of their instability in vapor atmosphere. Recently, Rivero-Crespo *et al.* synthesized a robust and highly crystalline MOF, which can stabilize Pt^+ single atom sites by a water cluster. The work reported a double water attack mechanism for the MOF to give CO_2, in which both oxygen atoms in CO_2 come from H_2O. However, the synthesis of the MOF is complex and time-consuming, requiring further development.[55]

The optimization of metal sites mainly focuses on adjusting the electronic structure by adjusting the surrounding environment. Regardless of the loaded metal sites or support metal sites, it is vital to reveal the volcano-type relationship between metal sites and surrounding atoms, which can provide a valid active site design reference for future research.

3.2 Carbon monoxide activation

Meanwhile, carbon monoxide activation is essential for CO elimination in WGSR. Sometimes, an oxygen vacancy can serve as a CO adsorption site at the interfacial zone between the loaded metal and supports. However, in most LT-WGSR processes, d-block elements such as noble metals can serve as effective CO activation sites by cooperating with the supports.[56,57] Opinions on how to optimize the activation sites for better performance remains unclear and contradictory. In this section, optimizing the geometric structure and electronic structure are considered as two feasible choices for the enhancement of d-block element performance (shown in Fig. 5), which will be discussed below.

3.2.1 Geometric structure. The geometric structure can directly affect the catalytic performance by changing the interaction between the catalysts and substrates. For instance, metal loaded on supports can be controllably synthesized with various sizes, such as nanoparticles, clusters and single atoms.[58] Based on the size effect, different sizes exhibited different catalytic performances and stabilities. In addition, the exposed facet of the catalysts is a key factor of the catalytic performance.[59] Thus, it is essential to summarize the merits and drawbacks of different geometric structures to provide clear strategies for reference.

Generally, it is well-known that with the single atom catalysts providing the largest quantity of interfacial sites, it should exhibit an increase in efficiency for WGSR. However, various studies have aimed to identify the active sites of CO activation and prove that nanoparticles performed better than single atoms by time-dependent infrared spectroscopy. The result proved that only CO adsorbed on Pt nanoparticles could be activated and participate in the reaction (demonstrated in Fig. 6a).[25] Therefore, with decent catalytic performance and stability, they have been widely investigated for LT-WGSR since 1996.[19,34] Andreas *et al.* designed TiO_2-supported Pt catalysts, and used density functional theory (DFT) calculations and microkinetic modeling to clarify the activity of the three-phase boundary. Their results suggested that the dominant catalytic process on $Pt_8/TiO_2(110)$ should be the redox pathway, and the better activity of the three-phase boundary can be correlated with the reduced CO adsorption energy on Pt sites and increased number of oxygen vacancies.[59] Moreover, Zhao *et al.* synthesized a Pt–TiO_2 composite with ultra-small Pt nanoparticles encapsulated in sub-50 nm hollow TiO_2 nanospheres. With the decrease of the Pt particle size, the catalyst shows a much higher turnover frequency (TOF) value, which can be attributed to the size-dependent variation in the electronic structure of the Pt species and the sintering prevention effect from TiO_2 encapsulation. This work provided a valid synthesis strategy for loading Pt on the internal surface of TiO_2 nanospheres, and revealed a creative catalyst design in which the deactivation of Pt could be avoided by controllable support encapsulation.[60] CeO_2 is a typical reducible support, and is frequently selected as the support of noble metals such as Au.[61] Fu *et al.* compared the activity of Au nanoparticles and clusters on CeO_2, and found that the abundant interfacial sites between Au clusters and CeO_2 induced superior catalytic performance when compared to Au nanoparticles during WGSR.[62] In short, the size of the loaded metals directly determines the number of active sites.

Zhang *et al.* synthesized Pt clusters and single atoms by changing the loaded facets shown in Fig. 6b. They closely investigated the CO adsorption on Pt by IR spectroscopy, as given in Fig. 6c. Zhang *et al.* proved that the binding energy between CO and Pt nanoparticles is weaker than that between CO and Pt single atoms by the blue shift of the PtO_4^{2+} peak compared with the $Pt^{\delta+}$ and Pt^0 peaks. This means that single atom catalysts (SACs) may show promising research value.[63] Therefore, for WGSR, single atom sites with appropriate geometry design can still effectively activate CO for further reaction with other intermediates, such as *OH. Lin *et al.* synthesized Ir_1/FeO_x SAC for WSGR, whose performance is one order of magnitude higher than its cluster and nanoparticle counterparts.[64] Furthermore, Liang *et al.* studied the redox

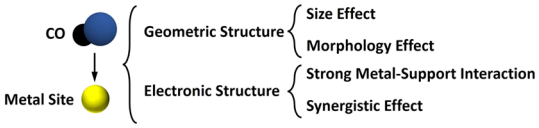

Fig. 5 Summary of the active site design for CO activation.

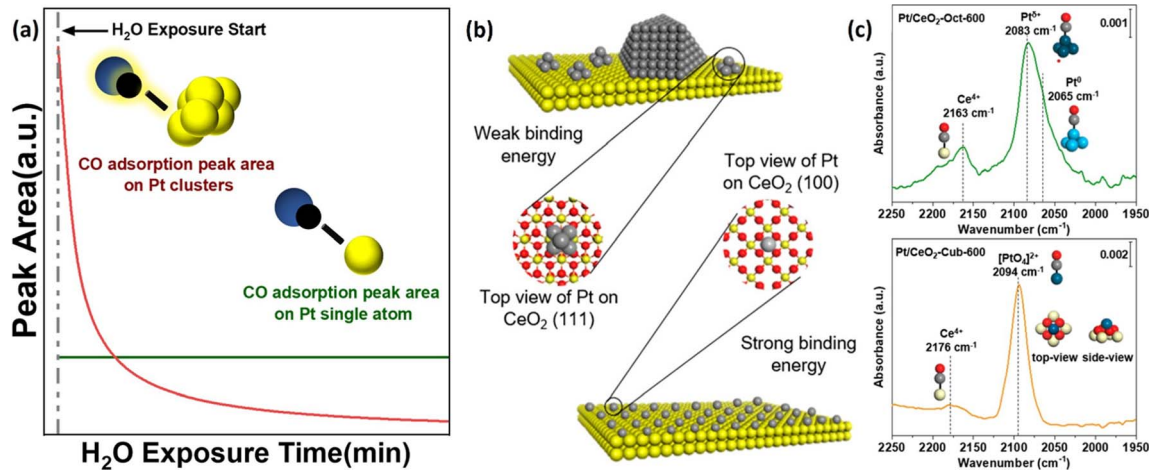

Fig. 6 (a) Time-dependent IR spectra of CO adsorbed on 1 wt% Pt/SiO_2 upon H_2O exposure. Peaks in the green zone correspond to CO adsorbed on Pt single atoms, and the peaks in blue zone correspond to CO adsorbed on Pt nanoparticles. Diagrams on the right side show the CO activation status on different sites. (b) Diagram of the Pt cluster and single atom on different CeO_2 facets. (c) *In situ* CO-DRIFTS of the Pt/CeO_2 samples, showing the bonding energy differences between CO and Pt with different sizes. Copyright © 2023, American Chemical Society.

mechanism of Ir_1/FeO_x for WGSR by detailed calculation and experiments, and proved that CO will be adsorbed and activated on the Ir single atom with a dual active site of Fe^{3+}–O···Ir^{2+}–O_v.65 Guan *et al.* (from the same group) also fabricated Rh_1/TiO_2 SAC, and obtained an overall CO conversion of ~95%. This showed that there are multiple choices of noble metal for LT-WGSR.[66] Some kinds of SACs have also broken the traditional model that noble metal sites are the actual CO activation sites. Sun *et al.* designed an Ir_1/α-MoC catalyst for LT-WGSR. Different from other works, they revealed that the great performance does not originate from the direct participation of Ir single atoms in the CO activation. The Ir single atoms served as a promoter that assisted Mo sites to activate CO. With kinetic measurements and theoretical calculation, they proved that the addition of Ir single atoms effectively changed the electronic property of Mo sites, resulting in an obvious reduction of the activation energy (E_a).[67] These works provide abundant possibilities for the utilization of SACs in future research studies with rational catalyst design to avert excessive adsorption.

As for the influence of exposed facets, Zhang *et al.* synthesized uniform cubic, dodecahedral and octahedral Cu nanocrystals by partial reduction of the Cu_2O nanocrystal. They found that the cubic Cu nanocrystal exposed (100) facets were more active than the dodecahedral Cu nanocrystal exposed (110) facets for H_2O dissociation and CO activation, and the octahedral Cu nanocrystal exposed (111) facets were inactive. By theoretical calculation results of the surface structures and H_2O adsorption energy change, it was confirmed that the formate species adsorbed on Cu (111) needed to overcome a large barrier to decompose, leading to the accumulation of formate and finally covering the active sites. Therefore, the Cu (111) facets are initially active, but is self-poisoned during the reaction.[68] On this basis, the research group studied ZnO/Cu in detail, and revealed that the catalysts would undergo an *in situ* restructuring process during WGSR to form the Cu-hydroxylated ZnO ensemble.[69] These results suggested that controlling the exposed facet of crystalized catalysts like traditional Cu-based catalysts might also be a potential strategy for performance optimization.

As shown above, a reasonable geometric structure is important to achieve better catalytic performance. The size and morphology effect should be investigated in detail and discussed based on prior experience and future works, with the goal of attaining some universal catalyst design rules.

3.2.2 Electronic structure

3.2.2.1 Strong metal-support interaction (SMSI). The strong metal-support interaction (SMSI) was first found by S. J. Tauster and S. C. Fung in 1978.[70] The interaction broadly exists in numerous kinds of supported catalysts and markedly adjusts their electronic structure, such as the electron states of loaded metals. For example, as we mentioned in the water dissociation section, SMSI can optimize the electron distribution of metal sites. Similarly, Abdel-Mageed *et al.* employed *operando* X-ray absorption spectroscopy (XAS) and FT-IR to identify the active Au species in the highly active Au/CeO_2 catalyst. By synthesizing the Au species with different electronic states ($Au^{\delta-}$, Au^0, $Au^{\delta+}$) on purpose, they presented an idea that the nanometer-sized Au^0 particles are the dominant active species rather than the cationic Au species (Au^{3+}).[71] Apart from that, the coordination number of active sites is related to the strength of SMSI. Jin *et al.* loaded Au atomic layers and isolated atoms on MoC to synthesize different Au/MoC catalysts. With XAS analysis and the catalytic performance test, they revealed a volcano-style pattern between the specific activity for LT-WGSR and the Au–Au coordination number. These results offered a reference for designing the geometric and electronic structure in the future.[72] The SMSI designed in these works showed that for better CO activation performance, there should be moderate interactions. Excessively weak SMSI cannot form satisfactory active sites, and the CO molecules cannot easily react with the oxygenate species if the SMSI is too strong.

To obtain an appropriate SMSI between loaded metals and supports, scientists offer a variety of methods. For example, Yang *et al.* demonstrated the origin of SMSI by using Pt/CeO_2 as a model catalyst and WGSR as a model reaction. On $CeO_2(110)$, Pt clusters embed into the CeO_2 lattice within 3–4 atomic layers. Such embedding structure optimizes the SMSI between the Pt clusters and CeO_2 to achieve more productive Pt sites.[73] Similarly, Pt/TiO_2 with an overlayer structure can also optimize the SMSI.[74] The results demonstrate that SMSI may be optimized by adjusting the geometric structure of the materials.

Another important factor of SMSI is the component and concentration of the active sites. Cu/Fe_3O_4 is a simple and non-toxic material. The formation of the $CuFe_2O_4$ spinel structure can enhance the thermostability, and change the electronic state of Cu and Fe by Jahn-Teller effect.[75] Lin *et al.* prepared a Cu/Fe_3O_4 catalyst by co-precipitation method to gain a larger amount of $CuFe_2O_4$, which was responsible for CO activation.[33] Han *et al.* further optimized the composition of Cu/Fe_3O_4 and found that $Cu_{0.3}Fe_{0.7}O_x$ exhibited the highest CO conversion. The group reported that an excessively loaded Cu will sinter and an insufficiently loaded Cu will suffer from a lack of active sites and poisoning.[12] Thus, future studies should determine the most applicable component for a promising material.

3.2.2.2 Synergistic effect. Besides normal nanoparticle-based materials, bimetallic sites and alloys have attracted much more attention. This is because the synergistic effect between two different metals is intriguing and contains profound scientific principles.[76,77] The recent research trend of bimetallic catalysts for WGSR focuses on adjustment of the bimetal size and optimization of the composition to reduce the cost and enhance the performance.[78–80] As typical active components, Cu and Ni can be simultaneously loaded on Fe_2O_3. The H_2-TPR results indicated that the SMSI occurs between the dopants (Cu or Ni) and Fe_2O_3, which is beneficial to LT-WGSR.[81] Zhang *et al.* anchored well-dispersed Pt single atoms on Co_3O_4 nanorods, forming a Pt_1Co_n/Co_3O_4 composite (structure schematic shown in Fig. 7b). They found that the singly dispersed Pt_1Co_n nanoclusters were the active sites of WGSR in the temperature range of 150–200 °C. After increasing the temperature to about 300 °C, Co_3O_4 (as demonstrated in Fig. 7a) will be reduced to CoO_{1-x} and Pt will sinter. This results in the formation of $Pt_mCo_{m'}/CoO_{1-x}$, as shown in Fig. 7c, with more abundant surface oxygen vacancies. Both H_2O dissociation and CO activation processes take advantage of the $Pt_mCo_{m'}$ active sites and achieve a lower activation energy, which suggested an effective method to tune the reactivity through reconstructing the oxide catalyst in the gas phase.[82] Xia *et al.* prepared Au and AuM (M = Ni, Cu, Pt) alloy nanoparticles supported on layered double hydroxides (LDHs). They found that Au_2Cu_1 exhibited the highest TOF value with modulation to the redox process at the interface of the AuM/LDHs interfaces.[83] These works on constructing bimetallic catalysts with optimized structure show great potential for LT-WGSR. However, the type and structure of the metals should be carefully designed to react in concert.

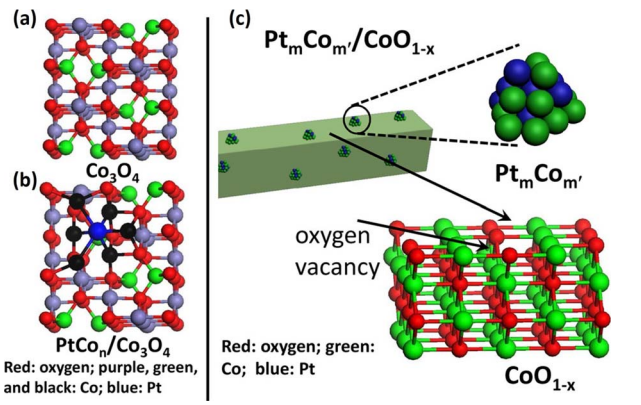

Fig. 7 Structural models of the surfaces of pure Co_3O_4 and active catalysts. (a) Top view of pure Co_3O_4. (b) Top view of Pt_1Co_n/Co_3O_4. (c) Diagrams of the synergistic active sites in $Pt_mCo_{m'}/CoO_{1-x}$. Copyright © 2013, American Chemical Society.

As a kind of electronic adjuvants, alkali elements are often doped in some supported catalysts to optimize the electronic structures of metal sites. Therefore, many notable works have been reported and provide a plethora of solutions. Au loaded on zeolites and mesoporous MCM-41 were found to be stabilized by the addition of Na^+ and K^+. The single site species of Au–$O(OH)_x$–(Na or K) are active for LT-WGSR below 200 °C. Furthermore, $AuO_{6-7}(OH)_2Na_9$ clusters exhibited the best catalytic performance and stabilization as shown by the applicable CO adsorption energy. This is because the addition of alkali ions served as an electron acceptor and shared part of the electrons being transferred to Au atoms to form a moderate Bader charge on Au.[84] Coincidentally, Pt–Na/SiO_2 was also synthesized and showed better activity than Pt/SiO_2 at temperatures below 300 °C.25 Kaftan *et al.* applied DRIFTS coupled with online quadrupole mass spectrometry (QMS) to observe the formation of surface species and demonstrate the enhancement of KOH-coated Pt/Al_2O_3. They assured that formates are the primary intermediate on uncoated Pt/Al_2O_3, while a film of hydroxides and carbonates is observed on the KOH-coated sample. It is interesting that changing the electronic structure by alkali species can affect the dominant reaction route of WGSR. Additionally, the strong red shift of the CO adsorption peak in DRIFTS suggested that K-coadsorption can weaken the C–O bond and strengthen the Pt–C bond, leading to the hindrance of CO desorption and facilitating the reaction of CO with *OH.[85] Ang *et al.* suppressed the formation of methane by covering a layer of Na/NaO_x on Ni-loaded CeO_2. The Na^+ replaces the Ce^{4+} in the lattice and generates abundant lattice defects, thus increasing the oxygen mobility, which will rapidly degrade the redundant CO adsorbed on Ni and prevent the self-poisoning of the catalyst.[86] These works revealed that alkali metal doping can change the electron distribution of catalysts, enhancing the performance of the active sites and changing the reaction route.

Generally, the electronic structure of active sites can be adjusted *via* the design of the bimetallic site and alkali doping based on the synergistic effect between the metals. For different sites with different performances, concrete analyses of their specific situations are necessary to ensure which elements can achieve the best optimization results.

4 Summary and prospect

WGSR is regarded as a promising reaction that can simultaneously fulfill the two expectations of converting CO and generating H_2. However, it is hindered by the fact that the temperature cannot synchronously overcome the thermodynamic and kinetic limits. Thus, many catalytic systems have been developed for high-efficiency WGSR. In this review, we considered WGSR as a combination of two half-reactions: H_2O dissociation and CO oxidation, which are the optimization targets of active site design. The combination of active site designs for the two side reactions makes it possible to achieve highly efficient WGSR for CO removal and H_2 production. In the past decade, numerous research studies have achieved important advances in the following prospects. For water dissociation, the concentration and structure of oxygen vacancies can be designed for better catalytic performance. Furthermore, the reasonable design of metal sites can help them efficiently participate in the process. For carbon monoxide activation that currently proceeds on d-block element sites, there are two valid options for designing first-class catalysts. This includes selectively synthesizing sites of suitable sizes and optimizing the electronic structure of the sites. Some catalysts have stood out with promising activity and industrial application potential, such as the loading of a noble metal on CeO_2, α-MoC. However, compared with relatively mature applied catalysts like the Cu/Zn/Al system, the harsh synthesis process and costly ingredients hindered their industrial application prospects. Further research studies should also examine how to reduce and minimize catalyst deterioration. Future design strategies for the active site should also take into consideration the industrial costs and production scenarios and specifically target economical, stable and efficient catalytic systems.

Taken together, although WGSR has been extensively investigated, there is still room for improvement of the catalytic systems. Thus, there is still much interest from the scientific community. With the proposal of more novel theories and the development of a large language model, the catalysts for WGSR must also stay up-to-date, and the designing methods can be assisted by AI prediction. We hope that the development of active site design for WGSR can help optimize H_2 generation and CO oxidation in the future.

Conflicts of interest

The authors declare no competing financial interests.

Data availability

No primary research results, software or code have been included and no new data were generated or analysed as part of this review.

Acknowledgements

This research was financially supported by the National Natural Science Foundation of China (No. 22421003) and the Strategic Priority Research Program (A) of the Chinese Academy of Sciences (XDA0390000).

References

1 L. Zhou, Y. Liu, S. Liu, H. Zhang, X. Wu, R. Shen, T. Liu, J. Gao, K. Sun, B. Li, *et al.*, For more and purer hydrogen-the progress and challenges in water gas shift reaction, *J. Energy Chem.*, 2023, **83**, 363–396, DOI: 10.1016/j.jechem.2023.03.055.

2 Z. Zhao, H. Ren, D. Yang, Y. Han, J. Shi, K. An, Y. Chen, Y. Shi, W. Wang, J. Tan, *et al.*, Boosting nitrogen activation via bimetallic organic frameworks for photocatalytic ammonia synthesis, *ACS Catal.*, 2021, **11**(15), 9986–9995, DOI: 10.1021/acscatal.1c02465.

3 G. Jacobs, P. M. Patterson, L. Williams, E. Chenu, D. Sparks, G. Thomas and B. H. Davis, Water-gas shift: in situ spectroscopic studies of noble metal promoted ceria catalysts for CO removal in fuel cell reformers and mechanistic implications, *Appl. Catal., A*, 2004, **262**(2), 177–187, DOI: 10.1016/j.apcata.2003.11.025.

4 K. Zhang, Q. Guo, Y. Wang, P. Cao, J. Zhang, M. Heggen, J. Mayer, R. E. Dunin-Borkowski and F. Wang, Ethylene carbonylation to 3-Pentanone with in situ hydrogen via a water-gas shift reaction on Rh/CeO_2, *ACS Catal.*, 2023, **13**(5), 3164–3169, DOI: 10.1021/acscatal.2c06123.

5 C. Ratnasamy and J. P. Wagner, Water gas shift catalysis, *Catal. Rev.*, 2009, **51**(3), 325–440, DOI: 10.1080/01614940903048661.

6 D. S. Newsome, The water-gas shift reaction, *Catal. Rev.*, 2006, **21**(2), 275–318, DOI: 10.1080/03602458008067535.

7 D.-W. Lee, M. S. Lee, J. Y. Lee, S. Kim, H.-J. Eom, D. J. Moon and K.-Y. Lee, The review of Cr-free Fe-based catalysts for high-temperature water-gas shift reactions, *Catal. Today*, 2013, **210**, 2–9, DOI: 10.1016/j.cattod.2012.12.012.

8 E. Baraj, K. Ciahotný and T. Hlinčík, The water gas shift reaction: catalysts and reaction mechanism, *Fuel*, 2021, **288**, 119817–119832, DOI: 10.1016/j.fuel.2020.119817.

9 J. Liu, R. Burciaga, S. Tang, S. Ding, H. Ran, W. Zhao, G. Wang, Z. Zhuang, L. Xie, Z. Lyu, *et al.*, Heterogeneous catalysis for the environment, *The Innovation Materials*, 2024, **2**(3), 100090, DOI: 10.59717/j.xinn-mater.2024.100090.

10 F. Meshkani and M. Rezaei, Promoted Fe_2O_3-Al_2O_3-CuO chromium-free catalysts for high-temperature water-gas shift reaction, *Chem. Eng. Technol.*, 2015, **38**(8), 1380–1386, DOI: 10.1002/ceat.201400668.

11 L. Foppa, T. Margossian, S. M. Kim, C. Muller, C. Coperet, K. Larmier and A. Comas-Vives, Contrasting the role of Ni/Al_2O_3 interfaces in water-gas shift and dry reforming of methane, *J. Am. Chem. Soc.*, 2017, **139**(47), 17128–17139, DOI: 10.1021/jacs.7b08984.

12 H. Yan, X.-T. Qin, Y. Yin, Y.-F. Teng, Z. Jin and C.-J. Jia, Promoted Cu-Fe_3O_4 catalysts for low-temperature water gas shift reaction: optimization of Cu content, *Appl. Catal. B Environ.*, 2018, **226**, 182–193, DOI: 10.1016/j.apcatb.2017.12.050.

13 J. Li, J. Chen, W. Song, J. Liu and W. Shen, Influence of zirconia crystal phase on the catalytic performance of Au/ZrO_2 catalysts for low-temperature water gas shift reaction, *Appl. Catal., A*, 2008, **334**(1–2), 321–329, DOI: 10.1016/j.apcata.2007.10.020.

14 D.-W. Jeong, H.-S. Na, J.-O. Shim, W.-J. Jang and H.-S. Roh, A crucial role for the CeO_2-ZrO_2 support for the low temperature water gas shift reaction over Cu-CeO_2-ZrO_2 catalysts, *Catal. Sci. Technol.*, 2015, **5**(7), 3706–3713, DOI: 10.1039/c5cy00499c.

15 M. V. Twigg and M. S. Spencer, Deactivation of supported copper metal catalysts for hydrogenation reactions, *Appl. Catal., A*, 2001, **212**(1–2), 161–174, DOI: 10.1016/s0926-860x(00)00854-1.

16 X. Lin, C. Chen, J. Ma, X. Fang, Y. Zhan and Q. Zheng, Promotion effect of Nb^{5+} for Cu/CeO_2 water-gas shift reaction catalyst by generating mobile electronic carriers, *Int. J. Hydrogen Energy*, 2013, **38**(27), 11847–11852, DOI: 10.1016/j.ijhydene.2013.07.001.

17 H. Jiang and J. Caro, Interfacial Au/MoC catalyst for low-temperature water-gas shift reaction, *Chem*, 2017, **3**(2), 209–210, DOI: 10.1016/j.chempr.2017.07.016.

18 K. Liu, Y. Li, L. Guo, Z. Zhang, L. Han, D. Zheng, X. Yang, Y. Zhang and W. Liao, Heralding the electrification era of catalysts: a highly practical current-assisted catalytic strategy, *Innovation*, 2025, **6**(4), 100804, DOI: 10.1016/j.xinn.2025.100804.

19 D. Andreeva, V. Idakiev, T. Tabakova and A. Andreev, low-temperature water-gas shift reaction over Au/α-Fe_2O_3, *J. Catal.*, 1996, **158**(1), 354–355, DOI: 10.1006/jcat.1996.0035.

20 H. Sakurai, A. Ueda, T. Kobayashi and M. Haruta, Low-temperature water-gas shift reaction over gold deposited on TiO_2, *Chem. Commun.*, 1997, (3), 271–272, DOI: 10.1039/a606192c.

21 Y. Chen, J. Lin and X. Wang, Noble-metal based single-atom catalysts for the water-gas shift reaction, *Chem. Commun.*, 2021, **58**(2), 208–222, DOI: 10.1039/d1cc04051k.

22 V. Palma, C. Ruocco, M. Cortese, S. Renda, E. Meloni, G. Festa and M. Martino, Platinum based catalysts in the water gas shift reaction: recent advances, *Metals*, 2020, **10**(7), 866, DOI: 10.3390/met10070866.

23 B. Qiao, A. Wang, X. Yang, L. F. Allard, Z. Jiang, Y. Cui, J. Liu, J. Li and T. Zhang, Single-atom catalysis of CO oxidation using Pt_1/FeO_x, *Nat. Chem.*, 2011, **3**(8), 634–641, DOI: 10.1038/nchem.1095.

24 L. Zhang, L. Han, H. Liu, X. Liu and J. Luo, Potential-cycling synthesis of single platinum atoms for efficient hydrogen evolution in neutral media, *Angew Chem. Int. Ed. Engl.*, 2017, **56**(44), 13694–13698, DOI: 10.1002/anie.201706921.

25 K. Ding, A. Gulec, A. M. Johnson, N. M. Schweitzer, G. D. Stucky, L. D. Marks and P. C. Stair, Identification of active sites in CO oxidation and water-gas shift over supported Pt catalysts, *Science*, 2015, **350**(6257), 189–192, DOI: 10.1126/science.aac6368.

26 D. B. Pal, R. Chand, S. N. Upadhyay and P. K. Mishra, Performance of water gas shift reaction catalysts: a review, *Renew. Sustain. Energy Rev.*, 2018, **93**, 549–565, DOI: 10.1016/j.rser.2018.05.003.

27 Y.-L. Lee, K.-J. Kim, G.-R. Hong and H.-S. Roh, Target-oriented water-gas shift reactions with customized reaction conditions and catalysts, *Chem. Eng. J.*, 2023, **458**, 141422, DOI: 10.1016/j.cej.2023.141422.

28 H. S. Taylor, A theory of the catalytic surface, *Proc. R. Soc. London, A*, 1925, **108**(745), 105–111, DOI: 10.1098/rspa.1925.0061.

29 M. Zhu and I. E. Wachs, Iron-based catalysts for the high-temperature water-gas shift (HT-WGS) reaction: A review, *ACS Catal.*, 2015, **6**(2), 722–732, DOI: 10.1021/acscatal.5b02594.

30 L. Huang, B. Han, Q. Zhang, M. Fan and H. Cheng, Mechanistic study on water gas shift reaction on the Fe_3O_4 (111) reconstructed surface, *J. Phys. Chem. C*, 2015, **119**(52), 28934–28945, DOI: 10.1021/acs.jpcc.5b09192.

31 J. Vecchietti, A. Bonivardi, W. Xu, D. Stacchiola, J. J. Delgado, M. Calatayud and S. E. Collins, Understanding the role of oxygen vacancies in the water gas shift reaction on ceria-supported platinum catalysts, *ACS Catal.*, 2014, **4**(6), 2088–2096, DOI: 10.1021/cs500323u.

32 K. Yu, L.-L. Lou, S. Liu and W. Z. Zhou, Asymmetric oxygen vacancies: the intrinsic redox active sites in metal oxide catalysts, *Adv. Sci.*, 2020, **7**(2), 1901970, DOI: 10.1002/advs.201901970.

33 X. Lin, R. Li, Y. Zhang, Y. Zhan, C. Chen, Q. Zheng and J. Ma, The role of surface copper species in Cu-Fe composite oxide catalysts for the water gas shift reaction, *Int. J. Hydrogen Energy*, 2015, **40**(4), 1735–1741, DOI: 10.1016/j.ijhydene.2014.11.105.

34 D. Andreeva, V. Idakiev, T. Tabakova, A. Andreev and R. Giovanoli, Low-temperature water-gas shift reaction on Au/α-Fe_2O_3 catalyst, *Appl. Catal., A*, 1996, **134**(2), 275–283, DOI: 10.1016/0926-860x(95)00208-1.

35 M. Yang, L. F. Allard and M. Flytzani-Stephanopoulos, Atomically dispersed Au-$(OH)_x$ species bound on titania catalyze the low-temperature water-gas shift reaction, *J. Am. Chem. Soc.*, 2013, **135**(10), 3768–3771, DOI: 10.1021/ja312646d.

36 H. Tang, H. Sun, D. Chen and X. Jiao, Fabrication of Pt/CeO_2 nanofibers for use in water-gas shift reaction, *Mater. Lett.*, 2012, **77**, 7–9, DOI: 10.1016/j.matlet.2012.02.122.

37 C. M. Kalamaras, K. C. Petallidou and A. M. Efstathiou, The effect of La^{3+}-doping of CeO_2 support on the water-gas shift reaction mechanism and kinetics over Pt/$Ce_{1-x}La_xO_{2-\delta}$, *Appl. Catal. B Environ.*, 2013, **136–137**, 225–238, DOI: 10.1016/j.apcatb.2013.02.003.

38 K. C. Petallidou and A. M. Efstathiou, Low-temperature water-gas shift on Pt/$Ce_{1-x}La_xO_{2-\delta}$: Effect of Ce/La ratio, *Appl. Catal. B Environ.*, 2013, **140–141**, 333–347, DOI: 10.1016/j.apcatb.2013.04.007.

39 P. Ebrahimi, A. Kumar and M. Khraisheh, A review of recent advances in water-gas shift catalysis for hydrogen production, *Emerg. Mater.*, 2020, **3**(6), 881–917, DOI: 10.1007/s42247-020-00116-y.

40 K. Yu, D. Lei, Y. Feng, H. Yu, Y. Chang, Y. Wang, Y. Liu, G.-C. Wang, L.-L. Lou, S. Liu, *et al.*, The role of Bi-doping in promoting electron transfer and catalytic performance of Pt/3DOM-$Ce_{1-x}BiO_{2-\delta}$, *J. Catal.*, 2018, **365**, 292–302, DOI: 10.1016/j.jcat.2018.06.025.

41 N. Liu, M. Xu, Y. Yang, S. Zhang, J. Zhang, W. Wang, L. Zheng, S. Hong and M. Wei, $Au^{\delta-}$-O_V-Ti^{3+} interfacial site: catalytic active center toward low-temperature water gas shift reaction, *ACS Catal.*, 2019, **9**(4), 2707–2717, DOI: 10.1021/acscatal.8b04913.

42 M. Xu, S. He, H. Chen, G. Cui, L. Zheng, B. Wang and M. Wei, TiO_{2-x}-modified Ni nanocatalyst with tunable metal-support interaction for water-gas shift reaction, *ACS Catal.*, 2017, **7**(11), 7600–7609, DOI: 10.1021/acscatal.7b01951.

43 M. Xu, S. Yao, D. Rao, Y. Niu, N. Liu, M. Peng, P. Zhai, Y. Man, L. Zheng, B. Wang, *et al.*, Insights into interfacial synergistic catalysis over Ni@TiO_{2-x} catalyst toward water-gas shift reaction, *J. Am. Chem. Soc.*, 2018, **140**(36), 11241–11251, DOI: 10.1021/jacs.8b03117.

44 Y. Li, M. Kottwitz, J. L. Vincent, M. J. Enright, Z. Liu, L. Zhang, J. Huang, S. D. Senanayake, W. D. Yang, P. A. Crozier, *et al.*, Dynamic structure of active sites in ceria-supported Pt catalysts for the water gas shift reaction, *Nat. Commun.*, 2021, **12**(1), 914, DOI: 10.1038/s41467-021-21132-4.

45 A. Chen, X. Yu, Y. Zhou, S. Miao, Y. Li, S. Kuld, J. Sehested, J. Liu, T. Aoki, S. Hong, *et al.*, Structure of the catalytically active copper-ceria interfacial perimeter, *Nat. Catal.*, 2019, **2**(4), 334–341, DOI: 10.1038/s41929-019-0226-6.

46 L. Lin, W. Zhou, R. Gao, S. Yao, X. Zhang, W. Xu, S. Zheng, Z. Jiang, Q. Yu, Y. W. Li, *et al.*, Low-temperature hydrogen production from water and methanol using Pt/α-MoC catalysts, *Nature*, 2017, **544**(7648), 80–83, DOI: 10.1038/nature21672.

47 T. Shao, L. Cao, L. Li, Y. Su, B. Hou, J. Lin and X. Wang, A noble-metal-free catalyst with MoC nanorod for low-temperature water gas shift reaction, *Chem. Eng. J.*, 2024, **485**, 149967, DOI: 10.1016/j.cej.2024.149967.

48 S. Yao, X. Zhang, W. Zhou, R. Gao, W. Xu, Y. Ye, L. Lin, X. Wen, P. Liu, B. Chen, *et al.*, Atomic-layered Au clusters on α-MoC as catalysts for the low-temperature water-gas shift reaction, *Science*, 2017, **357**(6349), 389–393, DOI: 10.1126/science.aah4321.

49 Y. Deng, Y. Ge, M. Xu, Q. Yu, D. Xiao, S. Yao and D. Ma, Molybdenum carbide: controlling the geometric and electronic structure of noble metals for the activation of O-H and C-H bonds, *Acc. Chem. Res.*, 2019, **52**(12), 3372–3383, DOI: 10.1021/acs.accounts.9b00182.

50 X. Zhang, M. Zhang, Y. Deng, M. Xu, L. Artiglia, W. Wen, R. Gao, B. Chen, S. Yao, X. Zhang, *et al.*, A stable low-temperature H_2-production catalyst by crowding Pt on alpha-MoC, *Nature*, 2021, **589**(7842), 396–401, DOI: 10.1038/s41586-020-03130-6.

51 J. A. Rodriguez, P. J. Ramirez, G. G. Asara, F. Vines, J. Evans, P. Liu, J. M. Ricart and F. Illas, Charge polarization at a Au-TiC interface and the generation of highly active and selective catalysts for the low-temperature water-gas shift reaction, *Angew Chem. Int. Ed. Engl.*, 2014, **53**(42), 11270–11274, DOI: 10.1002/anie.201407208.

52 J. A. Rodriguez, P. J. Ramírez and R. A. Gutierrez, Highly active Pt/MoC and Pt/TiC catalysts for the low-temperature water-gas shift reaction: effects of the carbide metal/carbon ratio on the catalyst performance, *Catal. Today*, 2017, **289**, 47–52, DOI: 10.1016/j.cattod.2016.09.020.

53 M. K. Gnanamani, G. Jacobs, W. D. Shafer, D. E. Sparks, S. Hopps, G. A. Thomas and B. H. Davis, Low temperature water-gas shift reaction over alkali metal promoted cobalt carbide catalysts, *Top. Catal.*, 2013, **57**(6–9), 612–618, DOI: 10.1007/s11244-013-0219-7.

54 M. Babucci, A. Guntida and B. C. Gates, Atomically dispersed metals on well-defined supports including zeolites and metal-organic frameworks: structure, bonding, reactivity, and Catalysis, *Chem. Rev.*, 2020, **120**(21), 11956–11985, DOI: 10.1021/acs.chemrev.0c00864.

55 M. A. Rivero-Crespo, M. Mon, J. Ferrando-Soria, C. W. Lopes, M. Boronat, A. Leyva-Perez, A. Corma, J. C. Hernandez-Garrido, M. Lopez-Haro, J. J. Calvino, *et al.*, Confined Pt_1^{1+} water clusters in a MOF catalyze the low-temperature water-gas shift reaction with both CO_2 oxygen atoms coming from water, *Angew Chem. Int. Ed. Engl.*, 2018, **57**(52), 17094–17099, DOI: 10.1002/anie.201810251.

56 L. DeRita, S. Dai, K. Lopez-Zepeda, N. Pham, G. W. Graham, X. Pan and P. Christopher, Catalyst architecture for stable single atom dispersion enables site-specific spectroscopic and reactivity measurements of CO adsorbed to Pt atoms, oxidized Pt clusters, and metallic Pt clusters on TiO_2, *J. Am. Chem. Soc.*, 2017, **139**(40), 14150–14165, DOI: 10.1021/jacs.7b07093.

57 P. Tepamatr, S. Charojrochkul and N. Laosiripojana, Water-gas shift activity over Ni/Al_2O_3 composites, *J. Compos. Sci.*, 2024, **8**(7), 239, DOI: 10.3390/jcs8070239.

58 X. M. Lai, Q. Xiao, C. Ma, W. W. Wang and C. J. Jia, Heterostructured ceria-titania-supported platinum catalysts for the water gas shift reaction, *ACS Appl. Mater. Interfaces*, 2022, **14**(6), 8575–8586, DOI: 10.1021/acsami.1c22795.

59 J.-W. An and G.-C. Wang, Titania crystal-plane-determined activity of copper cluster in water-gas shift reaction, *Appl. Surf. Sci.*, 2022, **591**, 153145, DOI: 10.1016/j.apsusc.2022.153145.

60 H. Zhao, S. Yao, M. Zhang, F. Huang, Q. Fan, S. Zhang, H. Liu, D. Ma and C. Gao, Ultra-small platinum nanoparticles encapsulated in sub-50 nm hollow titania nanospheres for low-temperature water-gas shift reaction, *ACS Appl. Mater. Interfaces*, 2018, **10**(43), 36954–36960, DOI: 10.1021/acsami.8b12192.

61 T. R. Reina, S. Ivanova, M. A. Centeno and J. A. Odriozola, The role of Au, Cu & CeO_2 and their interactions for an enhanced WGS performance, *Appl. Catal. B Environ.*, 2016, **187**, 98–107, DOI: 10.1016/j.apcatb.2016.01.031.

62 X. P. Fu, L. W. Guo, W. W. Wang, C. Ma, C. J. Jia, K. Wu, R. Si, L. D. Sun and C. H. Yan, Direct identification of active surface species for the water-gas shift reaction on a gold-ceria catalyst, *J. Am. Chem. Soc.*, 2019, **141**(11), 4613–4623, DOI: 10.1021/jacs.8b09306.

63 L. Zhang, Y. Niu, Y. Pu, Y. Wang, S. Dong, Y. Liu, B. Zhang and Z. W. Liu, In situ visualization and mechanistic understandings on facet-dependent atomic redispersion of platinum on CeO_2, *Nano Lett.*, 2023, **23**(24), 11999–12005, DOI: **10.1021/acs.nanolett.3c04008**.

64 J. Lin, A. Wang, B. Qiao, X. Liu, X. Yang, X. Wang, J. Liang, J. Li, J. Liu and T. Zhang, Remarkable performance of Ir_1/FeO_x single-atom catalyst in water gas shift reaction, *J. Am. Chem. Soc.*, 2013, **135**(41), 15314–15317, DOI: **10.1021/ja408574m**.

65 J. X. Liang, J. Lin, J. Liu, X. Wang, T. Zhang and J. Li, Dual metal active sites in an Ir_1/FeO_x single-atom catalyst: a redox mechanism for the water-gas shift reaction, *Angew Chem. Int. Ed. Engl.*, 2020, **59**(31), 12868–12875, DOI: **10.1002/anie.201914867**.

66 H. Guan, J. Lin, B. Qiao, S. Miao, A. Q. Wang, X. Wang and T. Zhang, Enhanced performance of Rh_1/TiO_2 catalyst without methanation in water-gas shift reaction, *AIChE J.*, 2016, **63**(6), 2081–2088, DOI: **10.1002/aic.15585**.

67 L. Sun, J. Xu, X. Liu, B. Qiao, L. Li, Y. Ren, Q. Wan, J. Lin, S. Lin, X. Wang, *et al.*, High-efficiency water gas shift reaction catalysis on α-MoC promoted by single-atom Ir species, *ACS Catal.*, 2021, **11**(10), 5942–5950, DOI: **10.1021/acscatal.1c00231**.

68 Z. Zhang, S. S. Wang, R. Song, T. Cao, L. Luo, X. Chen, Y. Gao, J. Lu, W. X. Li and W. Huang, The most active Cu facet for low-temperature water gas shift reaction, *Nat. Commun.*, 2017, **8**(1), 488–497, DOI: **10.1038/s41467-017-00620-6**.

69 Z. Zhang, X. Chen, J. Kang, Z. Yu, J. Tian, Z. Gong, A. Jia, R. You, K. Qian, S. He, *et al.*, The active sites of Cu-ZnO catalysts for water gas shift and CO hydrogenation reactions, *Nat. Commun.*, 2021, **12**(1), 4331, DOI: **10.1038/s41467-021-24621-8**.

70 S. Tauster, Strong metal-support interactions: occurrence among the binary oxides of groups IIA-VB, *J. Catal.*, 1978, **55**(1), 29–35, DOI: **10.1016/0021-9517(78)90182-3**.

71 A. M. Abdel-Mageed, G. Kučerová, J. Bansmann and R. J. Behm, Active Au Species During the Low-Temperature Water Gas Shift Reaction on Au/CeO_2: A Time-Resolved Operando XAS and DRIFTS Study, *ACS Catal.*, 2017, **7**(10), 6471–6484, DOI: **10.1021/acscatal.7b01563**.

72 C. Jin, B. Wang, Y. Zhou, F. Yang, S. Han, P. Guo, Z. Liu and W. Shen, Gold Atomic Layers and Isolated Atoms on MoC for the Low-Temperature Water Gas Shift Reaction, *ACS Catal.*, 2022, **12**(24), 15648–15657, DOI: **10.1021/acscatal.2c04651**.

73 J. Yu, X. Qin, Y. Yang, M. Lv, P. Yin, L. Wang, Z. Ren, B. Song, Q. Li, L. Zheng, *et al.*, Highly Stable Pt/CeO_2 Catalyst with Embedding Structure toward Water-Gas Shift Reaction, *J. Am. Chem. Soc.*, 2024, **146**(1), 1071–1080, DOI: **10.1021/jacs.3c12061**.

74 H. Wang, Y. Hui, Y. Niu, K. He, E. I. Vovk, X. Zhou, Y. Yang, Y. Qin, B. Zhang, L. Song, *et al.*, Construction of $Pt^{\delta+}$-O(H)-Ti^{3+} species for efficient catalytic production of hydrogen, *ACS Catal.*, 2023, **13**(15), 10500–10510, DOI: **10.1021/acscatal.3c02552**.

75 A. R. Tanna, U. N. Trivedi, M. C. Chhantbar and H. H. Joshi, Influence of Jahn-Teller Cu^{2+}(3d9) ion on structural and magnetic properties of Al-Cr co-substituted $CuFe_2O_4$, *Indian J. Phys.*, 2013, **87**(11), 1087–1092, DOI: **10.1007/s12648-013-0341-1**.

76 T. Yin, F.-Y. Meng, M. Zhang and Y.-W. Yan, Fabrication and characterization of nanoporous Ag-Pt alloy, *Rare Metals*, 2021, **40**(5), 1203–1207, DOI: **10.1007/s12598-020-01551-w**.

77 L. Liu and A. Corma, Bimetallic Sites for Catalysis: From Binuclear Metal Sites to Bimetallic Nanoclusters and Nanoparticles, *Chem. Rev.*, 2023, **123**(8), 4855–4933, DOI: **10.1021/acs.chemrev.2c00733**.

78 G. Chen, R. Gao, Y. Zhao, Z. Li, G. I. N. Waterhouse, R. Shi, J. Zhao, M. Zhang, L. Shang, G. Sheng, X. Zhang, X. Wen, L.-Z. Wu, C.-H. Tung and T. Zhang, Alumina-supported CoFe alloy catalysts derived from layered-double-hydroxide nanosheets for efficient photothermal CO_2 hydrogenation to hydrocarbons, *Adv. Mater.*, 2018, **30**(3), 1704663, DOI: **10.1002/adma.201704663**.

79 Y. Sato, K. Terada, Y. Soma, T. Miyao and S. Naito, Marked addition effect of Re upon the water gas shift reaction over TiO_2 supported Pt, Pd and Ir catalysts, *Catal. Commun.*, 2006, **7**(2), 91–95, DOI: **10.1016/j.catcom.2005.08.009**.

80 W. Srichaisiriwech and P. Tepamatr, Monometallic and Bimetallic Catalysts Supported on Praseodymium-Doped Ceria for the Water-Gas Shift Reaction, *Molecules*, 2023, **28**(24), 8146, DOI: **10.3390/molecules28248146**.

81 A. Jha, D.-W. Jeong, J.-O. Shim, W.-J. Jang, Y.-L. Lee, C. V. Rode and H.-S. Roh, Hydrogen production by the water-gas shift reaction using $CuNi/Fe_2O_3$ catalyst, *Catal. Sci. Technol.*, 2015, **5**(5), 2752–2760, DOI: **10.1039/c5cy00173k**.

82 S. Zhang, J. J. Shan, Y. Zhu, A. I. Frenkel, A. Patlolla, W. Huang, S. J. Yoon, L. Wang, H. Yoshida, S. Takeda, *et al.*, WGS catalysis and in situ studies of CoO_{1-x}, $PtCo_n/Co_3O_4$, and $Pt_mCo_{m'}/CoO_{1-x}$ nanorod catalysts, *J. Am. Chem. Soc.*, 2013, **135**(22), 8283–8293, DOI: **10.1021/ja401967y**.

83 S. Xia, L. Fang, Y. Meng, X. Zhang, L. Zhang, C. Yang and Z. Ni, Water-gas shift reaction catalyzed by layered double hydroxides supported Au-Ni/Cu/Pt bimetallic alloys, *Appl. Catal. B Environ.*, 2020, **272**, 118949, DOI: **10.1016/j.apcatb.2020.118949**.

84 M. Yang, S. Li, Y. Wang, J. A. Herron, Y. Xu, L. F. Allard, S. Lee, J. Huang, M. Mavrikakis and M. Flytzani-Stephanopoulos, Catalytically active $Au\text{-}O(OH)_x$-species stabilized by alkali ions on zeolites and mesoporous oxides, *Science*, 2014, **346**(6216), 1498–1501, DOI: **10.1126/science.1260526**.

85 A. Kaftan, M. Kusche, M. Laurin, P. Wasserscheid and J. Libuda, KOH-promoted Pt/Al_2O_3 catalysts for water gas shift and methanol steam reforming: an operando DRIFTS-MS study, *Appl. Catal. B Environ.*, 2017, **201**, 169–181, DOI: **10.1016/j.apcatb.2016.08.016**.

86 M. L. Ang, U. Oemar, E. T. Saw, L. Mo, Y. Kathiraser, B. H. Chia and S. Kawi, Highly active $Ni/xNa/CeO_2$ catalyst for the water-gas shift reaction: effect of sodium on methane suppression, *ACS Catal.*, 2014, **4**(9), 3237–3248, DOI: **10.1021/cs500915p**.